J Supercond Nov Magn (2013) 26:2515–2519
DOI 10.1007/s10948-012-1417-4

ORIGINAL PAPER

Sonochemical Synthesis and Magnetism in Co-doped ZnO Nanoparticles

Larisa B. Arruda · Douglas M.G. Leite · Marcelo O. Orlandi · Wilson A. Ortiz · Paulo Noronha Lisboa-Filho

Received: 17 November 2011 / Accepted: 5 January 2012 / Published online: 31 January 2012

Abstract The understanding and control of ferromagnetism in diluted magnetic semiconducting oxides (DMO) is a special challenge in solid-state physics and materials science due to its impact in magneto-optical devices and spintronics.

Several studies and mechanisms have been proposed to explain intrinsic ferromagnetism in DMO compounds since the theoretical prediction of room-temperature ferromagnetism. However, genuine and intrinsic ferromagnetism in 3d-transition metal-doped n-type ZnO semiconductors is still a controversial issue. Furthermore, for DMO nanoparticles, some special physical and chemical effects may also play a role.

In this contribution, structural and magnetic properties of sonochemically prepared cobalt-doped ZnO nanoparticles were investigated. A set of ZnO samples was prepared varying cobalt molar concentration and time of ultrasonic exposure. The obtained results showed that single phase samples can be obtained by the sonochemical method. However, cobalt nanoclusters can be detected depending on synthesis conditions. Magnetic measurements indicated a possible ferromagnetic response, associated to defects and cobalt substitutions at the zinc site by cobalt. However, ferromagnetism is depleted at higher magnetic fields. Also, an antiferromagnetic response is detected due to cobalt oxide cluster at high cobalt molar concentrations.

Keywords Dilute magnetic semiconductors · Co-doped zinc oxide · Magnetism

1 Introduction

Understanding high-temperature diluted magnetic semiconductors (DMS) is one of the leading problems in solid-state physics and materials science in this decade due to their promising applications in spintronic devices. Theoretical predictions suggest that ZnO is a strong candidate to DMS category, as well as GaN, both doped with manganese [1].

On the other side, the report on magnetism in HfO_2 undoped samples [2] has increased further discussion on ferromagnetism origin, now in oxides samples previously classified as diamagnetic. Even in ZnO pure, ferromagnetism was detected and associated to the presence of zinc vacancies in nano-powders [3].

High-temperature ferromagnetism is also reported for ZnO samples doped with different transition metals, such as Co [4–6], Mn [7, 8] and Cu [9], but the origin of this ferromagnetic behavior are under controversial discussion.

Some authors attribute the ferromagnetism found in DMS to 3d-transition metals when substituting the cation sites of the semiconductor host. This replacement strongly influences the electronic structure due to the strong hybridization among the 3d-orbital of magnetic ions and the matrix anions close to them, resulting in a strong magnetic interaction [10].

L.B. Arruda · D.M.G. Leite
POSMAT—Programa de Pós-Graduação em Ciência e Tecnologia de Materiais UNESP, Bauru, Brazil

M.O. Orlandi
Departamento de Físico-Química, Instituto de Química, UNESP Univ Estadual Paulista, Araraquara, Brazil

W.A. Ortiz
Departamento de Física, UFSCar Universidade Federal de São Carlos, São Carlos, Brazil

P.N. Lisboa-Filho (✉)
Departamento de Física, Faculdade de Ciências, UNESP Univ Estadual Paulista, Bauru, Brazil
e-mail: plisboa@fc.unesp.br

Another explanation for the observed ferromagnetic behavior is the possible formation of transition metal (MT) clusters highly affecting the obtained magnetic response [11].

Several are the synthesis routes to obtain nano-scale ZnO. Among the chemical routes there are the sol-gel method [12] and hydrothermal [13, 14], while for physical routes, it can be mentioned the ball milling process [15].

In this contribution the sonochemical method was used to obtain ZnO nanoparticles. In this method, the main phenomenon is the acoustic cavitation, which leads the formation, growth and collapse of bubbles in the liquid. The growth of cavitation bubbles occurs due to the diffusion of solute vapor in the volume of these bubbles, which are generated through the vibration movement of the ultrasonic waves. After the growth process, which will depend on the liquid and the wave frequency, the bubbles reach the final stage, where they collapse causing the breaking chemical bonds of the solute molecules [16]. Besides, bubbles into collapse can carry smaller particles, causing shocks among them, possible causing surface amorphization of the particles and also may resulting in the sintering of them. During this process, the extreme conditions generated at located points results temperature around 5000 °C, pressures of 1000 atm [17] and heating and cooling rates of 10^{11} K/s [16]. Such conditions give the samples unique characteristics such as decreasing of particles and high surface area [17].

In this paper, we report the preparation and the magnetic characteristics of ZnO samples doped with cobalt at concentrations of 2 and 10%. We focus the investigation of the magnetic responses from the insertion of Co^{2+} ions at the sites of Zn^{2+} ions, as well as those resulting from clusters formation, which were also analyzed by transmission electron microscopy (TEM).

2 Experimental Details

The ZnO:Co samples were obtained mixing ZnO (Aldrich, 99.99%) and CoO (Aldrich, 99.9%) in stoichiometric ratio in isopropyl alcohol (C_3H_8O), in order to obtain 0.5 g of each sample. The samples were then submitted to ultrasonic processing, in a Sonics brand model VCX-750, 750 Watts of power and frequency of 20 kHz for 5 hours, with pulses of 5 minutes and amplitude fixed at 70% from the nominal amplitude of the equipment. In the synthesis camera, the conditions were atmospheric air and the container with the samples and the ultrasonic tip were cooled with ice bath. At the end of each treatment, the samples were simply dried in an oven at 80 °C, and no heating treatment was performed.

The TEM images were obtained with Philips microscope model CM200, equipped with EDS detector (PGT). Magnetic measurements were performed in a XL Quantum Design SQUID Magnetometer.

3 Results and Discussion

As a reference, the structural properties of ZnO pure sample were still investigated without ultrasonic treatment. In Fig. 1 it is possible to note that the sample of pure commercial zinc oxide has a wide grain size distribution under submicrometer dimensions.

Figure 2 shows the TEM images for pure ZnO sample (a) and for nominally $Zn_{0,90}Co_{0,10}O$ sample (b) which was sonochemically treated by 5 hours of ultrasonic exposition.

For ZnO pure sample, in Fig. 2(a) it is possible to observe a non-homogeneous particle-size distribution. Thus, in Fig. 2(b) the reduction of particles is evidenced, although coexist together with these, particles with larger sizes, showing that despite the ultrasound cause the reduction of particles, this effect does not occur homogeneously throughout the sample, when used the time of 5 hours.

Furthermore, for the sample with 10% Co is already clearly observed the secondary phase formation with a different morphology from that identified as ZnO. The morphological differences can be noted in Fig. 3. X-Ray Energy Dispersion Spectroscopy (EDS) (not shown here) were performed and the particles of secondary phase identified as cobalt oxide. It is also possible to note that unlike for ZnO particles which present straight line and sharp shapes, as shown Fig. 3(a), the CoO particles present a more spherical and rough morphology, as can be seen in Fig. 3(b).

Another important verification of transmission microscopy measurements is that the ultrasonic treatment may induce the formation of an amorphous layer on the samples surface, as depicted in Fig. 4. The image on Fig. 4(a) shows a microscopy for pure ZnO and in (b) it is observed an amorphous layer around 3 nm thickness. It was not possible to observe the sintering of particles in any of the samples. More detailed studies are being carried out for determining the influence of this amorphization on the magnetic response of these samples.

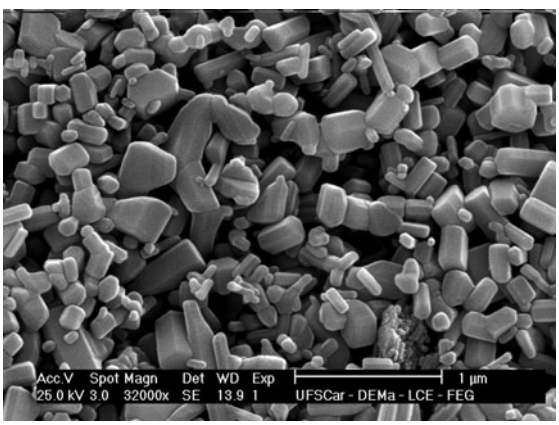

Fig. 1 Image obtained by (SEM) scanning electron microscope for pure ZnO sample without ultrasonic treatment

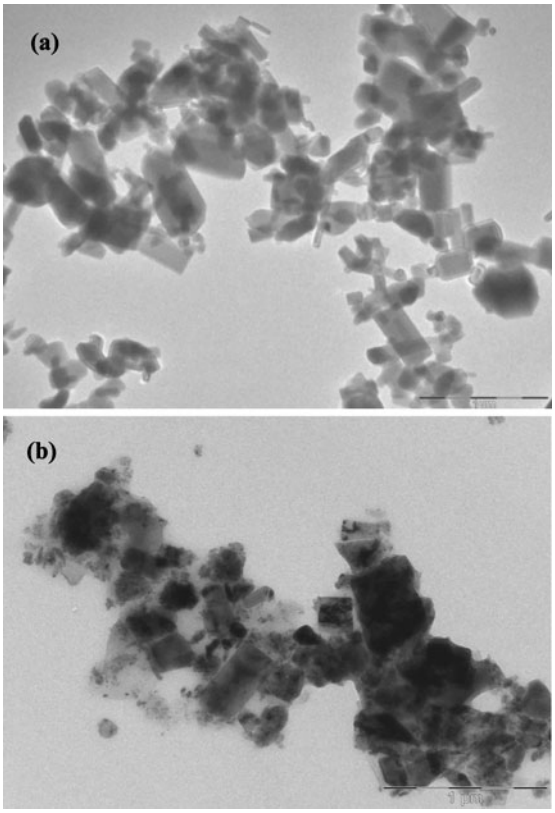

Fig. 2 Measurements of TEM for pure ZnO samples and $Zn_{0,90}Co_{0,10}O$. (**a**) without ultrasound the particle-size distribution is not homogeneous and larger than 200 nm. (**b**) with 5-hour ultrasound the particles suffer significant reduction making them more homogeneous in their size

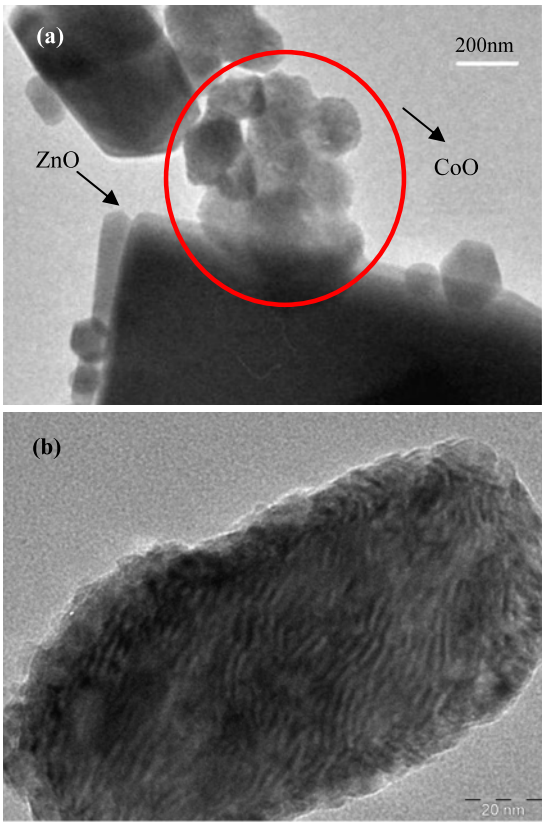

Fig. 3 TEM for $Zn_{0,90}Co_{0,10}O$ sample. (**a**) it is possible to observe the cluster formation of CoO and in (**b**) rough morphology of CoO quite different from the morphology of ZnO particles

Magnetization magnetic measurements (M) versus applied magnetic field (H) were performed on $Zn_{0.98}Co_{0.02}O$ and $Zn_{0.90}Co_{0.10}O$ samples at $T = 5$ and 300 K, as shown in Fig. 5. For both samples the magnetization showed a slight increase with decreasing temperature, this increase been higher for the sample with 10% Co.

The existence of hysteresis at lower field indicates that the powders present ferromagnetic response. For $Zn_{0.98}Co_{0.02}O$ sample, ferromagnetism may be related to Co^{2+} for Zn^{2+} substitution in ZnO matrix. Previous results obtained in our group indicated that the solubility limit in a sonochemical technique is close to 2%/mol for Co at ZnO lattice without secondary phase formation.

For $Zn_{0,90}Co_{0,10}O$ sample, a coercive field of 1400 Oe was observed, whereas for the sample doped with 2%, it was obtained a H_c of 1150 Oe, both at temperature of 5 K. At room temperature for the samples 2 and 10% Co coercive fields of 30 and 260 Oe were obtained, respectively.

Besides the ferromagnetic (FM) contribution, a strong antiferromagnetic (AF) and a weak paramagnetic (PM) contribution were also identified on the studied $M \times H$ curves. As shown in Fig. 6, all the tree contributions (PM, AF and FM) could be qualitatively described by a Brillouin function applied to different conditions [20]. In this work the magnetization (M) of each contribution was described by

$$M(H.T^{\mathrm{ef}}) = NgJ\mu_{\mathrm{B}}B_{J(y)} \tag{1}$$

with

$$B_J(y) = \frac{2J+1}{2J}\coth\left(\frac{2J+1}{2J}y\right) - \frac{1}{2J}\coth\left(\frac{1}{2J}y\right)$$

$$y = \frac{g\mu_{\mathrm{B}}JH}{k_{\mathrm{B}}T^{\mathrm{ef}}}$$

$$T^{\mathrm{ef}} = T + T_0$$

where N is the effective concentration of magnetic domain, g is the Landé factor, J is the total magnetic moment and μ_{B} is Bohr magneton. T^{ef} is the effective temperature with T_0 been positive to describe antiferromagnetism [19].

In this work the paramagnetic contribution was described by J between 2 and 7, with $T_0 = 0$ and $g = 2$. For the ferromagnetic contribution $J > 50$ with $T_0 = 0$ and $g = 2$, and the antiferromagnetic contribution $J = 2$, $T_0 > 10$ K and $g = 2$.

Single crystal and bulk ZnO present a weak diamagnetism with magnetic susceptibility close to 10^{-7} emu/gOe. In oxides nanoparticles, ferromagnetic behavior is detected

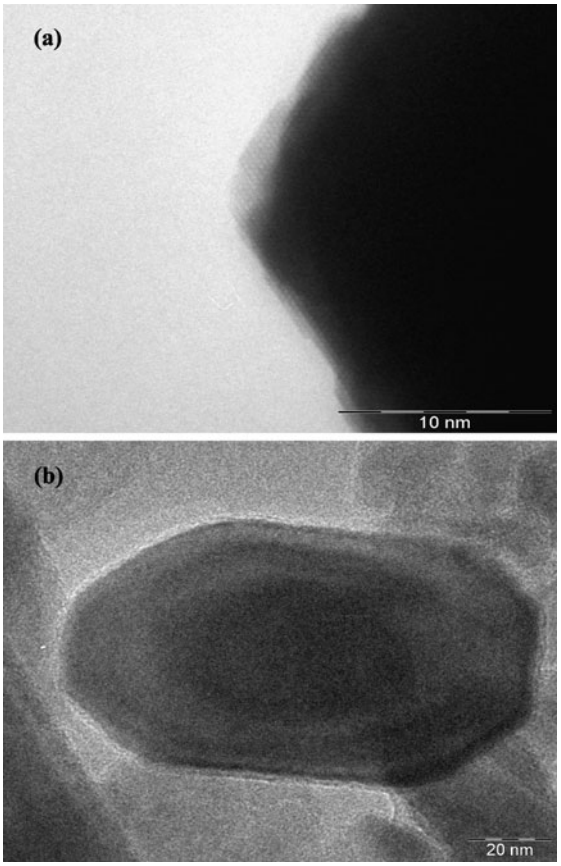

Fig. 4 Image obtained by TEM. (**a**) for pure ZnO sample without ultrasonic treatment and (**b**) for ZnO sample with ultrasonic treatment

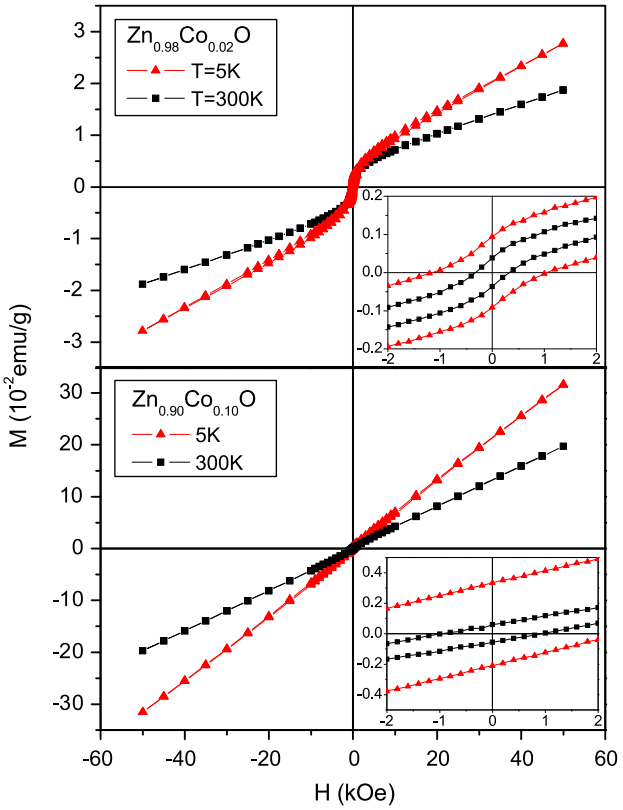

Fig. 5 $M \times H$ curves for $Zn_{0.98}Co_{0.02}O$ and $Zn_{0,90}Co_{0,10}O$ samples taken at $T = 5$ and 300 K, showing the existence of ferromagnetism

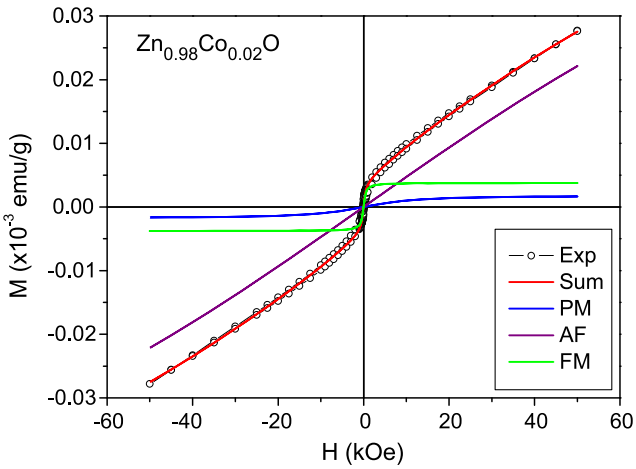

Fig. 6 Experimental $M \times H$ curve for ZnO sample doped with 2% Co taken at $T = 5$ K together with the adjusted contributions: paramagnetic, antiferromagnetic and ferromagnetic

and associated to point defects as oxygen and zinc vacancies (V_O and V_{Zn}, respectively) and even to interstitials oxygen and zinc ions (I_O and I_{Zn}, respectively). There are models in which Co^{2+}–V_O and Co^{2+}–I_{Zn} pairs act as magnetic centers for the long-range magnetic coupling.

Further, it is known that CoO nanoparticles present antiferromagnetic behavior associated to the antiferromagnetic structure of the particle core [18, 19]. However, depending on the particle sizes, also a ferromagnetic contribution may be detected due to the increase of the uncompensated moments at the disordered particle surface resulting from the reduced coordination of the surface spins. Therefore, for cobalt-doped samples, cobalt oxide clusters may also play a role in the ferromagnetic response.

In order to emphasize the FM contribution to the experimental $M \times H$ curve, we have plotted in Fig. 7 the experimental $M \times H$ data after subtracting the paramagnetic and antiferromagnetic contributions described by the Brillouin functions. The obtained curves make more evident the ferromagnetic behavior from prepared samples, mainly for doping of 10% Co, which presents coercive fields higher than 1000 Oe.

The ferromagnetic response found at studied samples may originate from exchange interactions between 3d levels of magnetic ions and p level of anions from semiconductor matrix, in this case oxygen. S-p hybridization is also pointed out as a possible cause of the ferromagnetic state at room temperature [10].

In summary, synthesis, morphological and magnetic characterization of $Zn_{0.98}Co_{0.02}O$ and $Zn_{0,90}Co_{0,10}O$ nano-

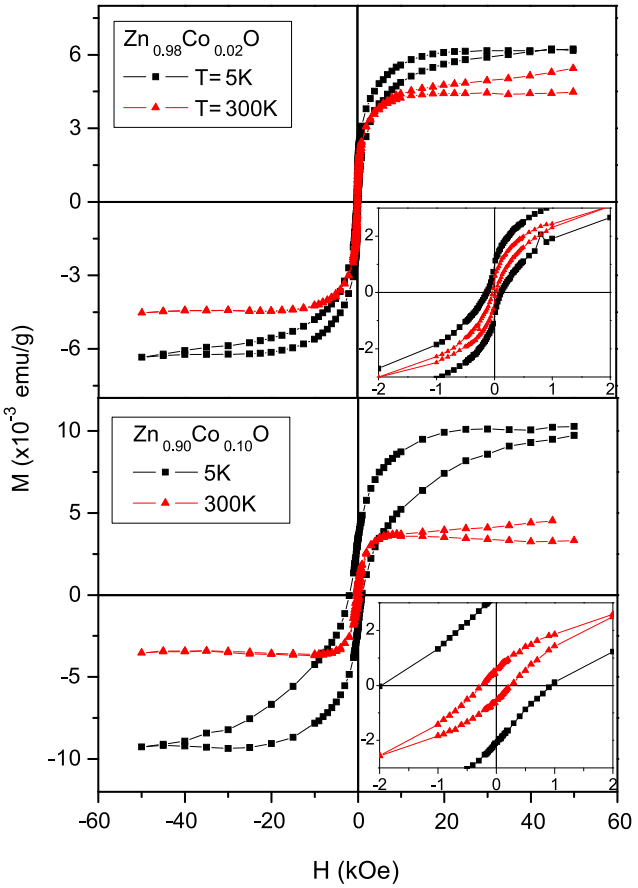

Fig. 7 Experimental $M \times H$ curves of Fig. 5 after the subtraction of the paramagnetic and antiferromagnetic contributions, demonstrating a further ferromagnetic response

metric samples in powder form were reported and obtained via sonochemical technique. The results indicated that with 5 hours of ultrasonic exposition, it has already been possible to note a significant decrease of particle average size. The formation of this CoO second phase was also confirmed by TEM images. Magnetic measurements showed that the studied samples present a ferromagnetic response. Subtraction of magnetic contributions through Brillouin function shows that this ferromagnetic response is suppressed mainly in high fields, where for 2% Co doping, the paramagnetism prevails. For 10% Co doping the antiferromagnetism is associated to CoO, which prevails in high fields masking the ferromagnetic response.

Acknowledgements The authors wish to thank Brazilian agencies FAPESP (research project 2009/14628-6 and 2006/05627-8) and CNPq (304810/2010-0) for financial support.

References

1. Dietl, T., Ohno, H., Matsukura, F., Cibert, J., Ferrand, D.: Science **287**, 1019 (2000)
2. Venkatesan, M., Fitzgerald, C., Coey, J.: Nature (London) **430**, 630 (2004)
3. Xu, Q., Zhou, S., Schmidt, H.: J. Alloys Compd. **487**, 665 (2009)
4. Boubekri, R., Beji, Z., Elkabous, K., Herbst, F., Viau, G., Ammar, S., Fiévet, F., Von Bardeleben, H.J., Mauger, A.: Chem. Mater. **21**, 843 (2009)
5. Lakshmi, Y.K., Srinivas, K., Sreedhar, B., Raja, M.M., Vithal, M., Reddy, P.V.: Mater. Chem. Phys. **113**, 749 (2009)
6. Wang, B., Xia, C., Iqball, J., Tang, N., Sun, Z., Lv, Y., Wu, L.: Solid State Sci. **11**, 1419 (2009)
7. Singhal, R.K., Dhawan, M.S., Gaur, S.K., Dolia, S.N., Kumar, S., Shripathi, T., Deshpande, U.P., Xing, Y.T., Saitovitch, E., Garg, K.B.: J. Phys. **153**, 012065 (2009)
8. Jayakumar, O.D., Salunke, H.G., Kadam, R.M., Mohapatra, M., Yaswant, G., Kulshreshtha, S.K.: Nanotechnology **17**, 1278 (2006)
9. Samanta, K., Bhattacharya, P., Katiyar, R.S.: J. Appl. Phys. **105**, 113929 (2009)
10. Liu, C., Yun, F., Morkoç, H.: J. Mater. Sci. **16**, 555 (2005)
11. Potzger, K., Kuepper, K., Xu, Q., Zhou, S., Schmidt, H., Helm, M., Fassbender, J.: J. Appl. Phys. **104**, 023510 (2008)
12. Azam, A., Ahmed, F., Arshi, N., Chaman, M., Naqvi, A.H.: J. Alloys Compd. **496**, 399 (2010)
13. Yu, L., Qu, F., Wu, X.: J. Alloys Compd. **504**, L1 (2010)
14. Baruah, S., Dutta, J.: Sci. Technol. Adv. Mater. **10**, 013001 (2009)
15. Lao, Y.W., Kuo, S.T., Tuan, W.H.: Ceram. Int. **35**, 1317 (2009)
16. Gedanken, A.: Ultrason. Sonochem. **11**, 47–55 (2004)
17. Suslick, K.S., Fang, M.M., Hyeon, T., Mdleleni, M.M.: Sonochem. Sonolumin. 291–320 (1999)
18. Dietl, T., Andrearczyk, T., Lipinska, A., Kiecana, M., Tay, M., Wu, Y.: Phys. Rev. B **76**, 155312 (2007)
19. Zhang, L., Xue, D., Gao, C.: J. Magn. Magn. Mater. **267**, 111 (2003)
20. Zajac, M., Gosk, J., Kaminska, M., Twardowski, A., Szyszko, T., Podsiadło, S.: Appl. Phys. Lett. **79**, 15 (2001)